*Journal of Engineering Science* *Vol. XXIX, no. 2 (2022), pp. 62 - 67*
*Fascicle* *Electronics and Computer Science* *ISSN 2587-3474*
*Topic* *Electronics and Communication* *eISSN 2587-3482*

**https://doi.org/10.52326/jes.utm.2022.29(2).06**
**UDC 621.37.001**

# THE INFLUENCE OF A RESIDUAL REFLECTIVITY AT THE FRONT FACET OF A MULTISECTION MASTER-OSCILLATOR POWER-AMPLIFIER

Eugeniu Grigoriev[1]*, ORCID: 0000-0002-0665-7500,
Vasile Tronciu[1], ORCID: 0000-0002-9164-2249,
Nils Werner[2], ORCID: 0000-0002-3055-6670,
Hans Wenzel[2], ORCID: 0000-0003-1726-022

[1]*Technical University of Moldova, 168 Stefan cel Mare Blvd., Republic of Moldova*
[2]*Ferdinand-Braun-Institut, Gustav-Kirchhoff-Straße 4, 12489 Berlin, Germany*
*Corresponding author: Eugeniu Grigoriev, *eugeniu.grigoriev@fiz.utm.md*

Received: 03. 05. 2022
Accepted: 04. 28. 2022

**Abstract.** This paper reports on the theoretical end experimental investigation of the output characteristics of a multisection master-oscillator power-amplifier (MOPA). It consists of a master oscillator (MO) composed by a gain section surrounded by two DBR sections monolithically integrated with a power amplifier (PA). We use a traveling wave equation model to calculate the optical output power in dependence on the current injected into the PA. The experimental results can be well explained with our theoretical analysis. For a finite front facet reflectivity of the PA the system is acting as a compound cavity.

**Keywords:** *distributed Bragg reflector laser, DBR, master oscillator power amplifier, MOPA, feedback.*

**Rezumat.** Articolul prezintă rezultatele finale ale investigației teoretice și experimentale a caracteristicilor de ieșire ale unui amplificator de putere master-oscilator multisecțional (MOPA). Amplificatorul este format dintr-un oscilator master (MO) compus dintr-o secțiune de câștig înconjurată de două secțiuni DBR integrate monolitic cu un amplificator de putere (PA). Este aplicat un model de ecuație a undelor de călătorie pentru a calcula puterea optică de ieșire în funcție de curentul injectat în PA. Rezultatele experimentale pot fi bine explicate prin analiza teoretică. Pentru o reflectivitate finită a fațetei frontale a PA, sistemul acționează ca o cavitate compusă.

**Cuvinte cheie:** *laser reflector Bragg distribuit, DBR, amplificator de putere master oscilator, MOPA, feedback.*

## Introduction

Over the last years, master oscillator power amplifiers have been requested by several applications such as LIDAR, free space optical communications, and spectroscopy. These applications need spatially diffraction limited and spectral narrow-band emission at several hundreds of milliwatts or even watts output power [1-4]. A monolithically integrated master oscillator power amplifier at 1.5 $\mu$m is presented in [2]. The three-section device includes a

distributed feedback (DFB) laser, a modulation section, and a high power tapered amplifier. In order to mitigate the coupling effects of the light reflected at the facets, the device has been designed with a bent cavity axis and a tilted waveguide at the front facet. Such devices emit more than 400 mW output power. The dynamical behavior of a 1.5-μm DFB tapered MOPA was reported in [3]. Three different emission regimes such as stable amplified DFB laser emission with wavelength jumps when sweeping the injection currents, multimode Fabry–Perot (FP) operation of the complete MOPA cavity, and self-pulsing operation at frequencies between 5 and 8 GHz were observed. In Ref. [4] the physical origins of these phenomena were investigated in the framework of a time-dependent travelling wave (TW) model which phenomenologically incorporates thermal effects via self and cross-heating of the different sections of the device similarly as proposed in [5] for the first time.

This paper is concerned with numerical and experimental investigations of a multisection monolithically integrated distributed Bragg reflector (DBR) MOPA emitting at 1120 nm using a TW model [5-8]. We report the output characteristics of such device varying the front facet reflectivity. In Section 2 we introduce the device under study and the theoretical model. Section 3 presents experimental and numerical results. Finally, conclusions are given in Section 4.

**Laser structure and equations**

A schematic representation of the multisection DBR MOPA device is shown in Figure 1. The MO consists of three sections. The gain section G having a length of 0.5 mm is complimented by 1 mm and 0.5 mm long DBR sections on left- and right-hand sides, respectively. The MO is connected to the 4 mm power amplifier PA. The reflectivity R at the front facet for the PA is varied from 0 to $10^{-1}$. The entire length of the device is 6 mm, and the emission wavelength is 1120 nm. The width of the ridge providing lateral fundamental mode operation is 4 μm. Electrical currents are injected into the gain section ($I_{MO}$) and the power amplifier ($I_{PA}$). The investigated structure is like to the one reported in [9]. The layer structure was grown by metalorganic vapor phase epitaxy. The active layer is formed by an InGaAs double quantum well which is embedded asymmetrically into a 4.8 μm thick vertical waveguide core [10, 11].

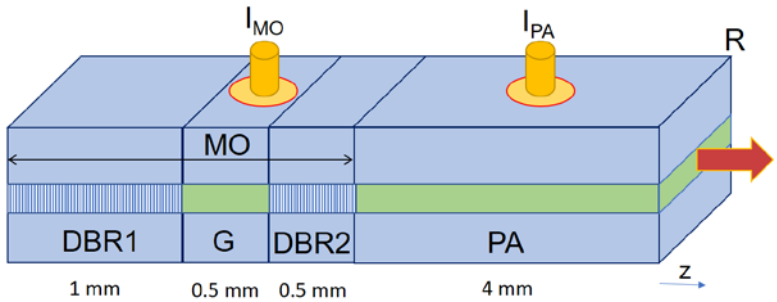


**Figure 1.** Setup of multisection DBR MOPA. The current injected into the MO is fixed. The current injected into the PA and the front facet reflectivity of the PA are varied.

The laser dynamics is analyzed using traveling wave equations for the slowly varying complex amplitudes $E^{+}(z,t)$ and $E^{-}(z,t)$ of the counter-propagating optical fields within each section of the device [7, 8] incorporated in [12]

$$\frac{n_g}{c_0}\frac{\partial}{\partial_t}E^{\pm} = [\mp\frac{\partial}{\partial_z} - i\Delta\beta(N,I)]E^{\pm} - i\kappa E^{\pm} + F_{sp}^{\pm} \quad (1)$$

where $c_0$ is the vacuum light speed and $\kappa$ is the field coupling coefficient due to the Bragg grating. We also use the rate equation for carrier density:

$$\partial_t N = \frac{I}{edWl_A} + \frac{U_F^{'}}{edr_s}\left(\overline{N} - N\right) - \left(\frac{N}{T} + BN^2 + CN^3\right), \\ -\frac{c_0}{n_g}\Re\sum_{\nu=\pm} E^{\nu *}\left[g(N) - D\right]E^{\nu} \tag{2}$$

where d and W are the thickness and width, respectively, of the active region. The relative propagation factor, the modal peak gain, and the change of the modal index with carrier density are given by following expressions

$$\Delta\beta = \delta_0 - i\frac{\alpha_0}{2} + k_0\left[\Delta n_N\left(N\right) + \Delta n_T\left(I\right)\right] + i\frac{g\left(N\right) - D}{2},$$

$$g(N) = \Gamma g' N_{tr} \ln\left(\frac{N}{N_{tr}}\right), \quad \Delta n_N = \tilde{\alpha}_H \frac{\Gamma g' N_{tr}}{k_0}\sqrt{\frac{N}{N_{tr}}}.$$

The values of main laser parameters used in our simulations are collected in Table 1. For a detailed description of the remaining model equations and parameters, we refer to [6-8].

*Table 1*

| Symbol | Description | Unit | Value |
|---|---|---|---|
| $\lambda_0$ | reference wavelength | m | $1.12 \cdot 10^{-6}$ |
| $L_G$ | length of active section | m | $0.5 \cdot 10^{-3}$ |
| $L_{DBR1}$ | length of DBR section | m | $1.0 \cdot 10^{-3}$ |
| $L_{DBR2}$ | length of DBR section | m | $0.5 \cdot 10^{-3}$ |
| $L_{PA}$ | length of PA section | m | $4.0 \cdot 10^{-3}$ |
| $R_r$ | rear facet intensity reflectivity | | 0 |
| $R_f$ | front facet intensity reflectivity | | 0···0.1 |
| $n_g$ | group refractive index | | 3.6 |
| $\kappa$ | coupling coefficient | $m^{-1}$ | $10 \cdot 10^{2}$ |
| $\alpha_H$ | linewidth enhancement factor | | -0,8 |
| $\alpha_0$ | internal absorption | $m^{-1}$ | $3 \cdot 10^{2}$ |
| Γ | optical confinement factor | | $0.68 \cdot 10^{-2}$ |
| g’ | differential gain | $m^2$ | $2555 \cdot 10^{-22}$ |
| $\varepsilon_g$ | gain compression factor | $m^3$ | $1 \cdot 10^{-24}$ |
| $N_{tr}$ | transparency carrier density | $m^{-1}$ | $1.5 \cdot 10^{-24}$ |
| *d* | thickness of active layer | m | $10 \cdot 10^{-9}$ |
| *W* | width of active layer | m | $4 \cdot 10^{-6}$ |
| *A* | recombination parameter | $s^{-1}$ | $3.4 \cdot 10^{-9}$ |
| *B* | recombination parameter | $m^3s^{-1}$ | $1.5 \cdot 10^{-16}$ |
| *C* | recombination parameter | $m^6s^{-1}$ | $5 \cdot 10^{-42}$ |
| $U'_F$ | derivative of Fermi level separation | V $m^3$ | $0.03 \cdot 10^{-24}$ |

**Results and discussions**

In what follows we discuss the output characteristics of the multisection device shown in Figure 1. We use the equations (1)-(2) and parameters listed in Table 1 for numerical calculations. The experiment was done at room temperature. Figure 2 illustrates both numerical and experimental output power versus injected current into PA characteristics for a fixed current of 200 mA injected into MO.

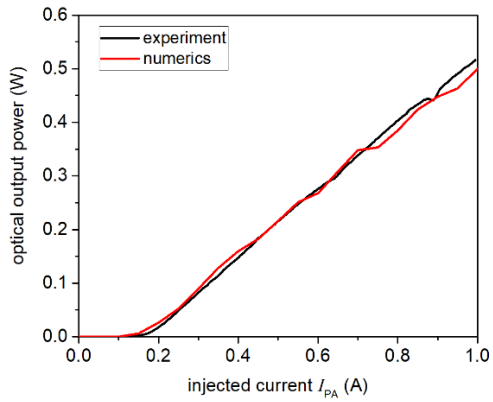


**Figure 2.** Dependence of output power on current injected into power amplifier PA: red – numerics, black – experiment. The current injected into the MO is 200 mA. The front facet reflectivity R =0.

From the characteristics a threshold of 0.15 A, and a slope of 0.6 W/A can be determined. The experimental investigations were performed at room temperature [9]. This figure indicated a good agreement between numerical calculations and experimental results. We next examine the same dependence as in Figure 2 what happens if the front facet reflectivity in increased to $10^{-2}$. Figure 3a shows the measured characteristics. As mentioned before, for zero reflectivity the threshold current is 0.16 A. On the other hand, an increase of front facet reflectivity reduces the threshold current to 0.09 A (red curve in Figure 3a). One can observe an increase of the slope to 0.78 W/A. This is due to the fact that for a finite front facet reflectivity the system acts as compound cavity. However, for high currents one observes undulations of the output power with injected current.

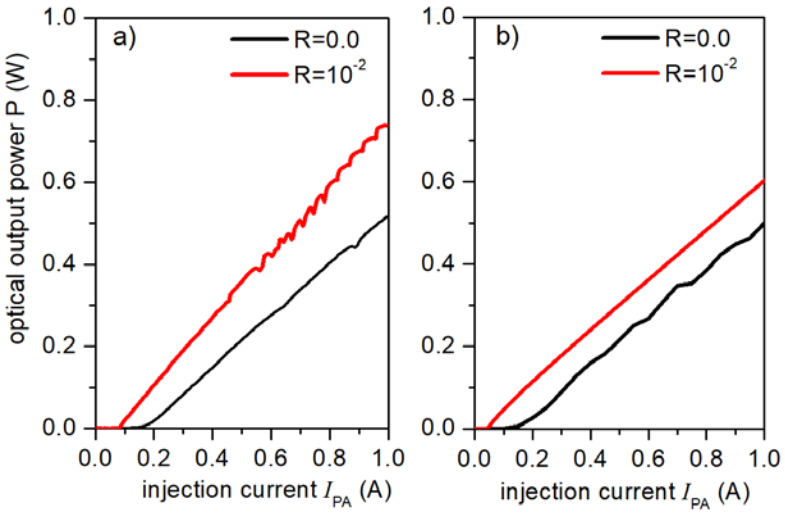


**Figure 3.** Output power versus injection current injected into the PA for two front facet reflectivities. The current injected into the MO is fixed to 200 mA: a) experiment, b) numerics.

Usually, this region with undulations is characterized by instabilities, which are not the subject of present investigations. The right panel of Figure 3 shows the numerically obtained results. We observe a good agreement between experiment and numerics regarding the decrease of the threshold current (0.05 A), However the slope (0.60 W/A) remains only constant in the simulation. In what follows, we show in Figure 4 how the front facet reflectivity affects the output power. An increase of the reflectivity from zero (black line) to $10^{-3}$ (red line) leads to a parallel shift of the characteristics to lower currents keeping the slope efficiency almost unaffected. A further increase of the front facet reflectivity to $10^{-1}$ remains the threshold current almost unchanged ($I_{th}$= 0.05 A) but reduces the slope to a value of 0.42 W/A due to a reduction of the outcoupled power.

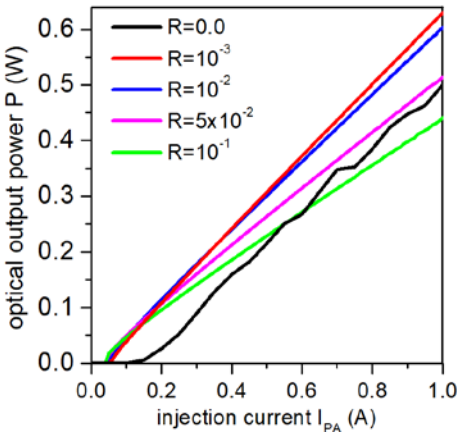


**Figure 4.** Simulated power–current characteristics for different front facet reflectivities.

## Conclusions

We have carried out experimental and theoretical investigations of the output characteristics of multisection master-oscillator power-amplifier. The MO is designed to be composed of a gain section and two DBR sections. Both simulations and experiment show a good quantitative agreement between output laser characteristics for zero front facet reflectivity. When the front facet reflectivity is increased the MOPA works as a compound cavity. We believe that our work provides a good basis for future study and provides some hints for more detailed investigations of mechanisms behind the MOPA effects.

**Acknowledgments:** This work was supported by the National Agency for Research and Development of Moldova within the project 20.80009.5007.08 *"Study of optoelectronic structures and thermoelectric devices with high efficiency"*. We thank M. Radziunas for providing his LDSL code.

**References**

1. Crump P., Brox O., Bugge F., Fricke J., Schultz C., Spreemann M., Sumpf B., Wenzel H., Erbert G. High power, high effciency monolithic edge-emitting GaAs-based lasers with narrow spectral widths. In: *Advances in Semiconductor Lasers*, 2012, No. 49.
2. Faugeron M. et al. High Power Three-section integrated master oscillator power amplifier at 1.5 µm. In: *IEEE Photonics Technology Letters*, Jul. 1st 2015, V. 27, No. 13, p. 1449
3. Vilera M., Pérez-Serrano A., Tijero J. M. G., Esquivias I. Emission Characteristics of a 1.5-µm All-Semiconductor tapered master oscillator power amplifier. In: *IEEE Photon. Journal*, Apr. 2015, V. 7, No. 2.
4. Perez-Serrano A., Vilera Mariafernanda, Javaloyes Julien, Tijero Jose Manuel G., Esquivias Ignacio, Baile Salvador Wavelength jumps and multimode instabilities in integrated master oscillator power amplifiers at 1.5 µm. Experiments and theory. In: *IEEE J. Sel. Top. Quantum. Electron.*, Nov./Dec. 2015, V. 21, No. 6, 1500909

5. Spreemann M., Lichtner M., Radziunas M., Bandelow U., Wenzel H. Measurement and simulation of distributed feedback tapered master oscillator power amplifiers. In: *IEEE J. Quantum Electron.*, 2009, 45(6), 609-616
6. Mindaugas R., Tronciu V., Bandelow U., Lichtner M., Spreemann M., Wenzel H. Mode transitions in distributed-feedback tapered master-oscillator power-amplifier: theory and experiments. In: *Opt Quant Electron* 2008, 40, 1103-1109
7. Radziunas M., Wünsche H. J. Multisection lasers: Longitudinal modes and their dynamics. In: J. Piprek, *Optoelectronic Devices*, 2005, Springer: New York, p. 121-150
8. Radziunas M.: Traveling wave modeling of nonlinear dynamics in multisection laser diodes', in: J. *Piprek (Ed.), Handbook of Optoelectronic Device Modeling and Simulation: Lasers, Modulators, Photodetectors, Solar Cells, and Numerical Methods,* 2017, V. 2, CRC Press, Ch. 31
9. Werner N., Wegemund J., Gerke S., Feise D., Bugge F., Paschke K., Tränkle G. Comparison of distributed Bragg reflector ridge waveguide diode lasers and monolithic master oscillator power amplifiers. In: *Proceedings SPIE,* Volume 105531D, 2018, Novel In-Plane Semiconductor Lasers XVII.
10. Paschke K., Wenzel H., Fiebig C., Blume G., Bugge F., Fricke J., Erbert G. High brightness, narrow bandwidth dbr diode lasers at 1120 nm. In: *IEEE Phot. Techn. Lett.*, 2013, No. 25 (20) 1951-1954
11. Bugge F., Erbert G., Fricke J., Gramlich S., Staske R., Wenzel H., Zeimer U., Weyers M. 12 W continuous-wave diode lasers at 1120 nm with InGaAs quantum wells". In: *Appl. Phys. Lett.*, 2001, No. 79 (13) 1965-1967.
12. A software package LDSL-tool. Longitudinal Dynamics of multisection Semiconductor Lasers. http://www.wias-berlin.de/software/ldsl.